An extended abstract for Heat Transfer in Nuclear Systems, 9th AIAA/ASME Joint Thermophysics and Heat Transfer Conference, San Francisco, CA, 5-8 June 2006

Multiphysics Thrust Chamber Modeling for Nuclear Thermal Propulsion

Ten-See Wang*
NASA Marshall Space Flight Center, Huntsville, Alabama, 35812
Gary Cheng†
University of Alabama, Birmingham, Alabama, 35294
Yen-Sen Chen‡
Engineering Sciences,Inc., Huntsville, Alabama, 35815

The objective of this effort is to develop an efficient and accurate thermo-fluid computational methodology to predict environments for a solid-core, nuclear thermal engine thrust chamber. The computational methodology is based on an unstructured-grid, pressure-based computational fluid dynamics formulation. A two-pronged approach is employed in this effort: A detailed thermo-fluid analysis on a multi-channel flow element for mid-section corrosion investigation; and a global modeling of the thrust chamber to understand the effect of heat transfer on thrust performance. Preliminary results on both aspects are presented.

I. Introduction

Nuclear thermal propulsion (NTP) can carry far larger payloads and reduce travel time of astronauts to Mars than is now possible with chemical propulsion. The feasibility of NTP engine systems was established by extensive testing in the Rover/NERVA programs and the technical merits of NTP have been identified in numerous studies and summarized.[1] For the solid-core NTP legacy engines tested during the Rover/NERVA era, heat transfer efficiency and degree of hydrogen dissociation are two important performance factors. Yet the impact of hydrogen dissociation on engine performance was not quantitatively identified. In addition, although the so-called flow element mid-section corrosion[2] was thought to be caused by the cracking of coating material and the materials development would remove that failure mode, detailed analysis is needed from a fundamental viewpoint to assess potential issues and enhancements. The objective of this effort is therefore to develop an efficient and accurate multiphysics thermo-fluid computational methodology to predict environments for a solid-core, NTP engine thrust chamber, with the emphasis on the effect of hydrogen dissociation on engine performance and investigation of the mid-section corrosion mode.

The current task scope is to develop and implement conjugate heat transfer and porosity modules based on an existing Unstructured-grid Navier-Stokes Internal-external computational fluid dynamics Code (UNIC), and to perform three-dimensional, multi-physics (real fluid, chemically reacting, turbulent flow, and conjugate heat transfer) thrust performance and heat transfer analyses for a solid-core, nuclear thermal engine thrust chamber, to provide thermal, fluid, and hydrogen environments. A two-pronged approach is employed in this effort: A detailed conjugate heat transfer analysis on a multi-channel flow element, and a global modeling of the thruster chamber with a porosity modeling technique. It is anticipated that the detailed analysis on a single flow element provides detailed fluid, thermal, and hydrogen environments for failure investigations, while the global thrust chamber analysis helps the understanding of the effect of heat transfer on thrust performance. These modeling activities will be validated as much as possible by testing performed by other related tasks.

---

*Technical Assistant, ER43, Thermal and Combustion Analysis Branch, Propulsion Structure, Thermal, and Fluids Analysis Division, Senior Member AIAA.
†Assistant Professor, Department of Mechanical Engineering, Member AIAA.
‡President, Member AIAA.

II. Computational Methodology

A. Computational Fluid Dynamics

The CFD methodology is based on a multi-dimensional, finite-volume, viscous, chemically reacting, unstructured grid, and pressure-based formulation. Time-varying transport equations of continuity, species continuity , momentum, total enthalpy, turbulent kinetic energy, and turbulent kinetic energy dissipation were solved using a time-marching sub-iteration scheme and are written as:

$$\frac{\partial \rho}{\partial t}+\frac{\partial}{\partial x_j}\left(\rho u_j\right)=0 \tag{1}$$

$$\frac{\partial \rho \alpha_i}{\partial t}+\frac{\partial}{\partial x_j}\left(\rho u_j \alpha_j\right)=\frac{\partial}{\partial x_j}\left[\left(\rho D+\frac{\mu_t}{\sigma_\alpha}\right)\frac{\partial \alpha_i}{\partial x_j}\right]+\omega_i \tag{2}$$

$$\frac{\partial \rho u_i}{\partial t}+\frac{\partial}{\partial x_j}\left(\rho u_j u_i\right)=-\frac{\partial p}{\partial x_i}+\frac{\partial \tau_{ij}}{\partial x_j} \tag{3}$$

$$\frac{\partial \rho H}{\partial t}+\frac{\partial}{\partial x_j}\left(\rho u_j H\right)=\frac{\partial p}{\partial t}+Q_r+\frac{\partial}{\partial x_j}\left(\left(\frac{K}{C_p}+\frac{\mu_t}{\sigma_H}\right)\nabla H\right)+\frac{\partial}{\partial x_j}\left(\left(\mu+\mu_t\right)-\left(\frac{K}{C_p}+\frac{\mu_t}{\sigma_H}\right)\right)\nabla\left(V^2/2\right)+\theta \tag{4}$$

$$\frac{\partial \rho k}{\partial t}+\frac{\partial}{\partial x_j}\left(\rho u_j k\right)=\frac{\partial}{\partial x_j}\left[\left(\mu+\frac{\mu_t}{\sigma_k}\right)\frac{\partial k}{\partial x_j}\right]+\rho\left(\Pi-\varepsilon\right) \tag{5}$$

$$\frac{\partial \rho \varepsilon}{\partial t}+\frac{\partial}{\partial x_j}\left(\rho u_j \varepsilon\right)=\frac{\partial}{\partial x_j}\left[\left(\mu+\frac{\mu_t}{\sigma_\varepsilon}\right)\frac{\partial \varepsilon}{\partial x_j}\right]+\rho\frac{\varepsilon}{k}\left(C_1\Pi-C_2\varepsilon+C_3\Pi^2/\varepsilon\right) \tag{6}$$

A predictor and corrector solution algorithm was employed to provide coupling of the governing equations. A second-order central-difference scheme was employed to discretize the diffusion fluxes and source terms. For the convective terms, a second-order upwind total variation diminishing difference scheme was used. To enhance the temporal accuracy, a second-order backward difference scheme was employed to discretize the temporal terms. Details of the numerical algorithm can be found in Ref's 3-7.

An extended k-ε turbulence model[8] was used to describe the turbulence. A modified wall function approach was employed to provide wall boundary layer solutions that are less sensitive to the near-wall grid spacing. Consequently, the model has combined the advantages of both the integrated-to-the-wall approach and the conventional law-of-the-wall approach by incorporating a complete velocity profile and a universal temperature profile[6]. A 2-species, 3-reaction detailed mechanism[9] was used to describe the hydrogen dissociation and recombination chemical kinetics.

B. Computational Conjugate Heat Transfer in Solids

The solid heat conduction equation is solved with the gas-side heat flux distributions as its boundary conditions. The solid heat conduction equation can be written as:

$$\frac{\partial \rho C T}{\partial t}-\frac{\partial}{\partial x_i}\left(\kappa\frac{\partial T}{\partial x_i}\right)=Q_v+Q_s \tag{7}$$

where Q_v and Q_s represent source terms from volumetric and boundary contributions, respectively. κ and C denote the thermal conductivity and capacity of the solid material, respectively. The temperature at the fluid-solid interface is obtained by enforcing the heat flux conservation condition.

C. Porosity Modeling

For the two-temperature porosity model, separate thermal conductivities for the flow and the solid parts are used. The heat transfer between the flow and solid is modeled by using the empirical correlation of heat transfer coefficient for circular pipes as a function of flow Reynolds number. Ergun's equation is used as a point of departure for the drag loss. An empirical multiplier for both the heat transfer and drag loss will be determined by comparing

solutions of flow passing through a porous flow element with those of a 19-channel flow element using detailed conjugate heat transfer modeling. The Continuity, Navier-Stokes and Energy (Total Enthalpy) Equations, can be written in a Cartesian tensor form with a porosity factor, α, included:

$$\frac{\partial \alpha\rho}{\partial t}+\frac{\partial}{\partial x_j}\left(\alpha\rho u_j\right)=0 \tag{8}$$

$$\frac{\partial \alpha\rho u_i}{\partial t}+\frac{\partial}{\partial x_j}\left(\alpha\rho u_j u_i\right)=-\alpha\frac{\partial p}{\partial x_i}+\alpha\frac{\partial \tau_{ij}}{\partial x_j}-L_\alpha \tag{9}$$

$$\frac{\partial \alpha\rho H}{\partial t}+\frac{\partial}{\partial x_j}\left(\alpha\rho u_j H\right)=\alpha\frac{\partial p}{\partial t}+Q_\alpha+\frac{\partial}{\partial x_j}\left(\alpha\frac{\mu}{P_r}\nabla H\right)+\frac{\partial}{\partial x_j}\left(\alpha\left(1-\frac{\mu}{P_r}\right)\nabla\left(V^2/2\right)\right) \tag{10}$$

For the solid heat conduction,

$$\frac{\partial(1-\alpha)\rho_s C_s T_s}{\partial t}=\frac{\partial}{\partial x_j}\left((1-\alpha)\kappa_s\nabla T_s\right)-Q_\alpha \tag{11}$$

where L_α and Q_α represent the drag loss and heat transfer source due to the porous material. Using the Ergun's equation for the drag loss,

$$L_\alpha=\rho(1-\alpha)\frac{1.75+150\dfrac{1-\alpha}{\mathrm{Re}_d}}{d\alpha^3}|U|\bullet u_i \tag{12}$$

For the heat exchange source term,

$$Q_\alpha=fA_\alpha H\left(T_s-T_g\right) \tag{13}$$

where H and A_α represent the heat transfer coefficient and wetted surface area between the gas and solid, respectively. Subscripts s and g denote the solid and gas domain, respectively. The remaining parameter on the right-hand-side of Eq. (13), f, is an empirical parameter to be determined by comparing solution of flow passing through a 19-channel fuel element using detailed conjugate heat transfer modeling and that of flow passing through a homogeneous fuel element with the effect of the 19-channel described by the porosity model.

III. Computational Grid Generation

Hybrid computational grids were generated using a software package GRIDGEN. A series of grid verification studies were performed to determine the current grid size. It is also found during the grid study that the computed gas-solid interface temperature is most stable when structured-grid layers are present on both sides of the interface.

IV. Boundary and Inlet Conditions

No-slip condition was applied to the solid walls. Fixed mass flow rate boundary condition was used at the inlet, and mass conservation boundary condition was used at the exit. The inlet conditions were obtained from system simulation for the Small Engine.

V. Results and Discussion

A. Preliminary power distribution for a single flow element

It is known that the power distribution inside a reactor normally resembles a Cosine curve with its peak at the center and reduces to a small value at the boundaries due to escaping neutrons. To model this effect numerically for a single, chamber-sized flow element, a section is implemented in the porous volume identification subroutine to define the boundary distances from the axis of peak power generation. This set of distances is then used to construct the Cosine distribution function. This method is good for fuel assembly regions with constant cross-sectional shape. An off-centered peak power input can be assigned.

Figures 1 and 2 show the predicted chamber temperature contours for a centered and an off-centered peak power distribution in a single porous flow element. The peak chamber temperatures for the two cases are about the same, but the location of the peak chamber temperature of the off-centered power distribution solution is shifted towards y = -2 cm location. Due to this shift in temperature profile, the density and velocity distributions also become biased. This in turn causes biased drag loss and pressure distributions in the porous region. As a result, side force is created. It is postulated that biased power distributions can end up with substantial side forces, which could be a contributing factor in flow element failures.

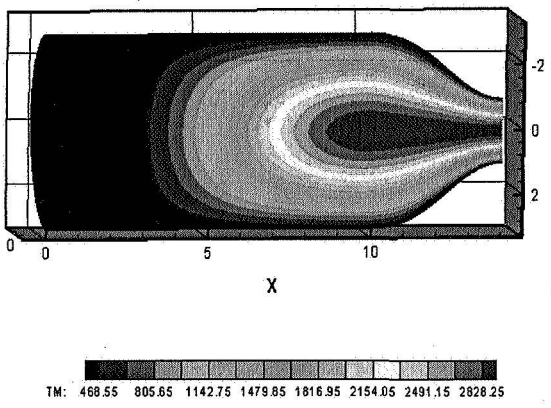

Fig. 1 Predicted chamber temperature contours with centered peak power in the porous flow element region from 3 to 10 cm.

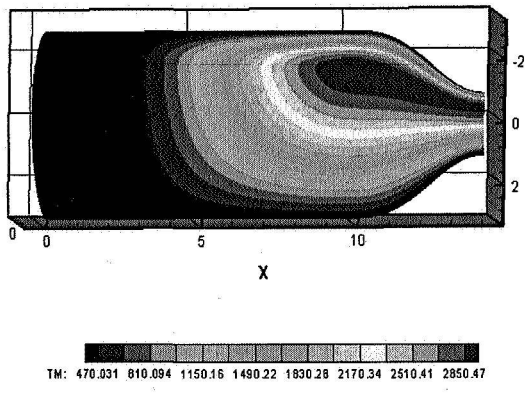

Fig. 2 Predicted chamber temperature contours with peak power off-centered (along y = -2 cm and z = 0 cm axis).

B. Initial 3-D grids for a detailed 19-channel flow element

Figure 3 shows the surface grid representation for the web of a 19-channel flow element. Figure 4 shows a detailed grid representation of the web and hot flow channels. Flow solutions for a series of fixed outer wall temperatures will be performed in order to validate the heat transfer equation for the porosity model. Flow solutions for different channel diameters at 2.03, 2.29 and 2.54 mm will also be performed to anchor the drag law for the porosity model.

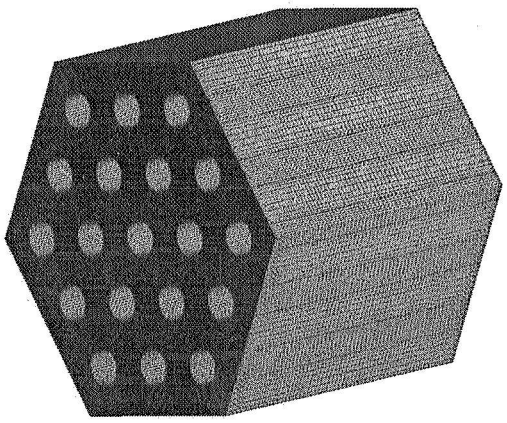

Fig. 3 Surface grid representation for the web of a 19-channel flow element.

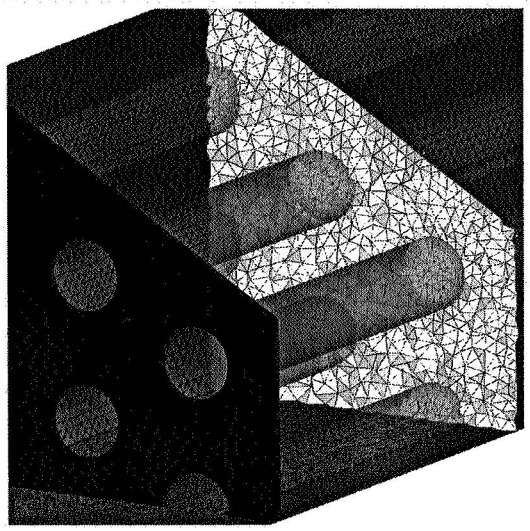

Fig. 4 Detailed grid representation of a quarter of a fuel element.

VI. Conclusions

An efficient and accurate multiphysics thermo-fluid computational methodology is being developed to predict environments for a solid-core, NTP engine thrust chamber, to study the effect of hydrogen dissociation on engine performance and investigation of the mid-section corrosion mode. A two-pronged approach is employed in this effort: A detailed conjugate heat transfer analysis on a multi-channel flow element, and a global modeling of the thruster chamber with a porosity modeling technique. It is anticipated that the detailed analysis on a single flow element provides detailed fluid, thermal, and hydrogen environments for better understanding of the mid-section corrosion phenomenon, while the global thrust chamber analysis helps the understanding of the effects of heat transfer and hydrogen dissociation on thrust performance.

Acknowledgments

This study was partially supported by a Nuclear Systems Office task entitled "Multiphysics Thrust Chamber Modeling".

References

[1]Koenig, D.R., "Experience Gained from the Space Nuclear Rocket Program (Rover)," LA-10062-H, Los Alamos National Laboratory, Los Alamos, New Mexico, 1986.

[2]Lyon, L.L., "Performance of (U,Zr)C-Graphite (Composite) and of (U,Zr)C (Carbide) Fuel Elements in the Nuclear Furnace 1 Test Reactor," LA-5398-MS, Los Alamos Scientific Laboratory, Los Alamos, New Mexico, 1973.

[3]Chen, Y.-S., Liu, J., Zhang, S., and Mallapragada, P., "An Integrated Tool for Launch Vehicle Base-Heating Analysis," Final Report, NAS8-00002, Engineering Sciences, Inc., Huntsville, AL, 2001.

[4]Chen. Y.-S., Zhang S., and Liu, J., "Stage Separation Performance Analysis Project," Final Report, H-34345D, Engineering Sciences, Inc., Huntsville, AL, 2002.

[5]Wang, T.-S., Chen, Y.-S., Liu, J., Myrabo, L.N., and Mead, F.B. Jr., "Advanced Performance Modeling of Experimental Laser Lightcraft," *Journal of Propulsion and Power,* **18**, 1129-1138 (2002).

[6]Wang, T.-S., "Multidimensional Unstructured-Grid Liquid Rocket Engine Nozzle Performance and Heat Transfer Analysis," AIAA Paper 2004-4016, 40th AIAA/ASME/SAE/ASEE Joint Propulsion Conference, Fort Lauderdale, Florida, 2004.

[7]Wang, T.-S., "Transient 3-D Analysis of Nozzle Side Load in Regeneratively Cooled Engines," AIAA Paper 2005-3942, 41st AIAA/ASME/SAE/ASEE Joint Propulsion Conference, Tucson, Arizona, 2005.

[8]Chen, Y.-S., and Kim, S. W., "Computation of Turbulent Flows Using an Extended k-ε Turbulence Closure Model," NASA CR-179204, 1987.
[9]Wang, T.-S., "Thermophysics Characterization of Kerosene Combustion," *Journal of Thermophysics and Heat Transfer*, **15**, 140-147 (2001).